Fermionic functional renormalization group investigation of Luttinger liquids

Roman Krčmár and Michael Weyrauch*
Physikalisch-Technische Bundesanstalt, Braunschweig, Germany
(Received 29 September 2011; revised manuscript received 8 March 2012; published 6 April 2012)

Luttinger-liquid parameters are extracted from ground-state energy calculations using a fermionic functional renormalization group (fRG) scheme similar to that proposed by Andergassen *et al*. [Phys. Rev. B **73**, 045125 (2006)]. A different way of interaction renormalization is proposed and compared to the method in this reference. The proposed new interaction renormalization produces superior numerical results for chemical potential as well as compressibility, while the Luttinger parameter K is obtained quantitatively similar in both interaction renormalization schemes. It is demonstrated that a consistent extraction of Luttinger-liquid parameters from the numerically calculated ground state within fRG meets several severe numerical issues, partly related to the fact that the truncated fRG is not a conserving approximation.

DOI: 10.1103/PhysRevB.85.155113 PACS number(s): 71.10.Pm

I. INTRODUCTION

The theoretical understanding of one-dimensional (1D) fermionic quantum systems stems mostly from bosonization and conformal field theory.[1,2] It was shown that in 1D the Fermi-liquid concept of quasifree fermions, which proved to be so enormously successful in higher dimensions, breaks down and must be replaced by the Luttinger-liquid (LL) concept of quasifree bosons.[3] Within a bosonized theory, the spectrum and correlation functions can be expressed in terms of a few basic Luttinger-liquid parameters, and correlation functions can be shown to decay algebraically at large distances.[1] The power-law exponents of the correlation functions may be related to the parameters which determine the finite-size dependence of the low-energy spectrum of the Luttinger-liquid Hamiltonian using conformal field theory.[2,4]

Effects of impurities in LL may be studied using renormalization group techniques[5,6] or, alternatively, conformal field theory methods using boundary operators.[7] Again, the scaling dimensions of boundary operators can be related to the finite-size scaling properties of the low-energy spectrum. The predictions of bosonization and conformal field theory in conjunction with the renormalization group analysis can be compared to microscopic models using exact methods such as Bethe ansatz or high-precision numerical methods such as DMRG.[8–10]

More recently, a new fermionic method, the functional renormalization group (fRG),[11–14] has been advocated as a useful tool for the description of one-dimensional Fermi systems.[15] This microscopic method allows calculations of correlation functions for rather large inhomogeneous systems with and without spin degrees of freedom. As a consequence, determination of impurity exponents is possible, a goal at present hardly achievable with other methods. In a series of papers, Luttinger-liquid parameters were extracted from the power-law decay of various correlation functions.[16,17] The necessary approximations in the fRG procedure were chosen judiciously for this purpose. Furthermore, in Refs. 16 and 17, the Luttinger-liquid parameter K, which characterizes the strength of interactions in a homogeneous LL, was related to the renormalized interactions of the fermionic system using the Luttinger model.

The purpose of this paper is to look at the fRG description of Luttinger liquids from a different perspective than the papers cited above. Here, we want to assess how well various fRG approximation schemes describe the finite-size structure of the ground-state energy. As was pointed out above, the finite-size dependence of a Luttinger liquid is determined by the same Luttinger-liquid parameters as the correlation functions. While the fRG procedure developed in Refs. 16 and 17 certainly was not designed with this goal in mind, in view of the conformal symmetry of the one-dimensional system under consideration, a consistent approach should be able to describe the ground state along with the impurity exponents. It is not our goal here to advocate fRG as a particularly precise and/or competitive way to calculate ground-state energies of Luttinger liquids, but rather to study the consistency of the (truncated) fRG in view of symmetries and conservation laws using Luttinger systems as an example.

It is well known[18] that due to the necessary truncations, the fRG procedure is not particle number conserving. Nonconserving approximations may lead to inconsistencies in the determination of the number of particles.[19] However, the functional renormalization group is a grand canonical method and, therefore, formulated for fixed chemical potential. Since we want to study systems at various filling factors, we need a procedure to determine the chemical potential for given fillings. Except at half-filling, the chemical potential must be determined numerically within the fRG approach, which proves to be a significant source of numerical uncertainty. This can be partly related to the nonconserving character of the fRG procedure.

In order to assess the precision of various fRG approximations, we compare fRG results with Bethe ansatz[20] calculations and perturbative results of Ref. 21. Already, second-order perturbation theory allows a good description of the finite-size scaling properties of the ground-state energy of a one-dimensional Fermi system. From these results, Luttinger-liquid parameters can be extracted with good precision as was demonstrated by comparison with exact Bethe ansatz calculations and high-precision numerical DMRG results.

We determine the ground-state energy using fRG using different approximation schemes. In addition to the special vertex approximation studied in Refs. 16 and 17, we investigate

a new renormalization scheme for the interaction. This renormalization scheme is consistently formulated in coordinate space for a finite system, while the interaction renormalization in Refs. 16 and 17 is done for an infinite system in Fourier space for momenta on the Fermi surface only. From the finite-size scaling properties of the ground-state energy, we then determine the Luttinger-liquid properties.

The article is organized as follows. In Sec. II, the fermionic model is defined, and LL theory is reviewed for our purposes. In Sec. III, we describe the details of our functional renormalization group (fRG) method. In particular, the new interaction renormalization scheme is described and compared to the scheme of Ref. 16. In Sec. IV, we present our numerical ground-state calculations and analyze them in terms of LL theory. A summary is presented in Sec. V.

II. ONE-DIMENSIONAL ELECTRON RING

A one-dimensional ring of interacting spinless fermions is modeled by the lattice Hamiltonian

$$H = \sum_{j=1}^{L}[-t(e^{-i\varphi/L}c_j^+c_{j+1} + e^{i\varphi/L}c_{j+1}^+c_j) + Uc_j^+c_jc_{j+1}^+c_{j+1}], \quad (1)$$

and we assume periodic boundary conditions $c_{L+1}^{(+)} = c_1^{(+)}$ for the electron creation and destruction operators c_j^+ and c_j, respectively. The number of possible electron sites on the ring is L; the ring is assumed to be filled with N electrons, i.e., the filling factor is given by $n_f = N/L$. The hopping amplitude t is set to 1 in the following in order to set the energy scale. The ring is threaded by a magnetic flux φ described by the Peierls' factor $e^{-i\varphi/L}$, and the electrons interact via nearest-neighbor density-density interactions with strength U.

At small enough interaction U, a system described by the Hamiltonian (1) enters the Luttinger-liquid phase. Using bosonization[3] and conformal symmetry arguments,[4] it can be shown that to order $1/L$ the ground-state energy of a Luttinger liquid without impurity can be written in the form

$$E_0 = \epsilon_0 L + \frac{\pi u}{2L}\left[-\frac{1}{3} + \frac{1}{K}N^2 + K\left(J - \frac{\varphi}{\pi}\right)^2\right] \quad (2)$$

with $J = 0$ for odd number of particles and $J = \pm 1$ for even number of particles ($J = +1$ for positive flux and $J = -1$ for negative flux). Therefore, the ground-state energy can be characterized by three basic parameters: the energy per site ϵ_0, the Luttinger-liquid parameters K, and the velocity u. The parameter K characterizes the interaction strength: $K = 1$ for noninteracting particles, $K > 1$ for attractive interactions, and $K < 1$ for repulsive interactions. The Luttinger-liquid parameters must be calculated from a microscopic model using analytical methods (e.g., Bethe ansatz) or numerically (e.g., DMRG). In the following, we will use such methods in order to benchmark the fRG calculations.

The magnetic flux induces a persistent electronic current I, which can be determined from the ground-state energy by differentiation with respect to magnetic flux $I = -\frac{\partial E_0}{\partial \varphi}$ due to the Hellmann-Feynman theorem.[22] From Eq. (2), one obtains

$$I = \frac{uK}{L}\left(J - \frac{\varphi}{\pi}\right). \quad (3)$$

Obviously, the sign of the persistent current depends on the parity of number of particles.

In previous studies of LL systems using fRG,[16,17] the LL parameters were extracted from the correlation functions. Here, we want to extract them from the finite-size scaling properties of the ground-state energy (2) assuming that the system enters the LL regime within the parameter regime considered here.

III. FUNCTIONAL RENORMALIZATION GROUP

In this section, we briefly explain our functional renormalization scheme and point out differences and relations to previous work.[17,23,24] Our scheme is similar to the setup in Ref. 24, however, here we include the interaction renormalization and correct details of the derivation of flow equations. The flow equations for the self-energies agree with results given in Refs. 23 and 24. However, the flow equation for the nearest-neighbor interaction has not been considered previously in this form.

The effective average action $\Gamma_k[\phi^*,\phi]$ for a fermionic many-body system fulfills the exact renormalization group equation[11,25]

$$\frac{\partial}{\partial k}\Gamma_k[\phi^*,\phi] = -\frac{1}{2}\mathrm{Tr}\left\{\left[\Gamma_k^{(2)}[\phi^*,\phi] + \mathbf{R}_k\right]^{-1}\frac{\partial \mathbf{R}_k}{\partial k}\right\}. \quad (4)$$

Here, $\Gamma_k^{(2)}$ is the inverse propagator as defined more explicitly in the Appendix, $\mathbf{R}_k$ is a suitable cutoff function, and $\phi(\tau) = (\phi_1(\tau), \ldots, \phi_L(\tau))$ an L-component Grassmann field, which depends on the imaginary time τ. In order to solve this functional differential equation, we introduce an approximation in terms of an effective potential U_k, i.e., we prescribe that the functional allowed for the effective average action is given by

$$\Gamma_k[\phi^*,\phi] = \int_0^\beta d\tau \sum_{j=1}^{L}\phi_j^*(\tau)\frac{\partial}{\partial\tau}\phi_j(\tau) + U_k(\phi^*(\tau),\phi(\tau)). \quad (5)$$

In particular, the effective potential does *not* depend on derivatives of the Grassmann fields $\phi(\tau)$. This assumption restricts the form of U_k to polynomials in the Grassmann fields ϕ:

$$U_k(\phi^*,\phi) = a_{0;k} + \sum_{i,j=1}^{L} a_{ij;k}\phi_i^*\phi_j + \sum_{i,j,l,m=1}^{L} a_{ijlm;k}\phi_i^*\phi_j\phi_l^*\phi_m + \ldots. \quad (6)$$

The coefficients $a_{;k}$ of the Grassmann polynomials are called "running couplings." By inserting this expansion of the effective average action on both sides of Eq. (4), one obtains a generally infinite set of differential equations for the running couplings. This set must be suitably truncated in order to be manageable.

To this end, we neglect couplings beyond those written out explicitly above in Eq. (6). While the truncation is necessary in order to keep the set of equations manageable, a problematic consequence is that the theory becomes nonconserving.[18] In order to further simplify, we assume that the nearest-neighbor interaction in the Hamiltonian (1) will only renormalize into nearest-neighbor couplings, i.e., does not lead to longer-range effective couplings due to renormalization. This leads to the following ansatz for the effective potential:

$$U(\phi^*,\phi) = a_{0;k} + \sum_{j=1}^{L} a_{jj,k}\phi_j^*\phi_j + a_{j,j+1;k}\phi_j^*\phi_{j+1} + a_{j,j-1;k}\phi_j^*\phi_{j-1} + \sum_{j=1}^{L} U_{j;k}\phi_j^*\phi_j\phi_{j+1}^*\phi_{j+1}. \quad (7)$$

Finally, we Fourier transform the Grassmann fields, using

$$\phi_j(\tau) = \frac{1}{\sqrt{\beta}}\sum_n e^{i\omega_n\tau}\phi_{j;n}, \quad \phi_j^*(\tau) = \frac{1}{\sqrt{\beta}}\sum_n e^{-i\omega_n\tau}\phi_{j;n}^* \quad (8)$$

with the Matsubara freuencies $\omega_n = (2n+1)\pi/\beta$, and only extract equations for the Fourier components $\phi_{j;0}$. This truncation is called *static approximation*.[26] In this approximation and for a special choice of the cutoff function $\mathbf{R}_k$ (given in the Appendix), we obtain the following set of differential equations for the various couplings (details of the derivation are presented in the Appendix): (i) for the ground-state energy $E_0 = a_0 + \mu N$,

$$\dot{a}_{0,k} = \frac{1}{\pi}\mathrm{Re}\left[\ln\det\left(\frac{1}{k}\mathbf{g}^{-1}(ik)\right)\right]; \quad (9)$$

(ii) for the self-energies,

$$\begin{aligned}\dot{a}_{ii;k} &= \frac{1}{\pi}\mathrm{Re}[U_{i-1;k}\mathbf{g}_{i-1,i-1}(ik) + U_{i;k}\mathbf{g}_{i+1,i+1}(ik)],\\ \dot{a}_{i+1,i;k} &= -\frac{U_{i;k}}{2\pi}[\mathbf{g}_{i+1,i}(ik) + \mathbf{g}_{i,i+1}^*(ik)],\\ \dot{a}_{i,i+1;k} &= -\frac{U_{i;k}}{2\pi}[\mathbf{g}_{i,i+1}(ik) + \mathbf{g}_{i+1,i}^*(ik)] = \dot{a}_{i+1,i;k}^*;\end{aligned} \quad (10)$$

(iii) and for the effective interaction,

$$\begin{aligned}\dot{U}_{i;k} = &-\frac{1}{2\pi}\left\{U_{i;k}^2\mathbf{g}_{i,i+1}(ik)\mathbf{g}_{i,i+1}^*(ik) + U_{i;k}^2\mathbf{g}_{i+1,i}^*(ik)\mathbf{g}_{i+1,i}(ik)\right\} - \frac{1}{\pi}\mathrm{Re}\left\{U_{i;k}^2\mathbf{g}_{i,i+1}(ik)\mathbf{g}_{i+1,i}(ik) - U_{i;k}^2\mathbf{g}_{i,i}(ik)\mathbf{g}_{i+1,i+1}(ik)\right.\\ &+ U_{i-1;k}U_{i,k}\mathbf{g}_{i-1,i}(ik)\mathbf{g}_{i,i-1}(ik) + U_{i;k}U_{i+1;k}\mathbf{g}_{i+1,i+2}(ik)\mathbf{g}_{i+2,i+1}(ik) + U_{i-1;k}U_{i+1;k}\mathbf{g}_{i-1,i+2}(ik)\mathbf{g}_{i+2,i-1}(ik)\\ &\left.- U_{i;k}^2\mathbf{g}_{i,i}^*(ik)\mathbf{g}_{i+1,i+1}(ik)\right\}.\end{aligned} \quad (11)$$

The overdot indicates a derivative with respect to k and $\mathbf{g}_{lm}^{-1}(ik) = (a_{lm;k} + ik\delta_{lm})$. While the propagator matrix $\mathbf{g}$ is a full matrix, only its band diagonal part is actually necessary for the solution of the flow equations.

For the solution of the set of coupled ordinary differential equations given above, one needs the following set of initial conditions. They are derived from the Hamiltonian (1) in the Appendix:

$$a_{0;k_0} = \tfrac{1}{4}LU - \tfrac{1}{2}L\mu, \quad (12)$$

$$a_{ii;k_0} = U - \mu, \quad (13)$$

$$a_{i,i+1;k_0} = -e^{-i\phi/L}, \quad (14)$$

$$a_{i+1,i;k_0} = -e^{i\phi/L}, \quad (15)$$

$$U_{i;k_0} = U, \quad (16)$$

where k_0 is a large but finite constant from which the renormalization flow starts. The initial flow from $k=\infty$ to k_0 is already included in the initial conditions given above. For a chain *without* impurity, the above large set of coupled differential equations simplifies considerably due to translational symmetry. In particular, the matrices $\mathbf{g}^{-1}$ acquire a Toeplitz form. For such matrices, determination of the determinant and inverse is easily possible as explained in the Appendix. We define $\rho_k \equiv a_{ii;k}$ and $\alpha_k \equiv a_{i,i+1;k}$ and obtain the following set of four coupled differential equations: (i) for the ground-state energy,

$$\dot{a}_0 = \frac{1}{2\pi}\sum_{m=1}^{L}\ln\left[1 + \frac{1}{k^2}(\rho_k + 2\,\mathrm{Re}\beta_{k,m})^2\right]; \quad (17)$$

(ii) for the self-energies,

$$\dot{\rho}_k = \frac{2U_k}{\pi}\mathrm{Re}\,P_k(0), \quad \dot{\alpha}_k = -\frac{U_k}{2\pi}[P_k(-1) + P_k^*(1)]; \quad (18)$$

(iii) and for the effective interaction,

$$\dot{U}_k = -\frac{U_k^2}{\pi}\left(\frac{1}{2}P_k(-1)P_k^*(-1) + \frac{1}{2}P_k(1)P_k^*(1) - P_k(0)P_k^*(0) + \mathrm{Re}\left[3P_k(-1)P_k(1) - P_k^2(0) + P_k(3)P_k(-3)\right]\right) \quad (19)$$

with

$$P_k(m) = \frac{e^{-im\varphi_k}}{(ik+\rho_k)\sqrt{1-\frac{1}{A_k^2}}}\left(O_k^{|m|} + O_k^m\frac{O_k^L e^{-iL\varphi_k}}{1 - O_k^L e^{-iL\varphi_k}} + O_k^{-m}\frac{O_k^L e^{iL\varphi_k}}{1 - O_k^L e^{iL\varphi_k}}\right). \quad (20)$$

For an infinite system, Eq. (20) simplifies to

$$P_k(m) = \frac{O_k^{|m|}}{(ik+\rho_k)\sqrt{1-\frac{1}{A_k^2}}}. \quad (21)$$

We have used the following abbreviations $\beta_{k,m} = \alpha_k \exp(im\frac{2\pi}{L})$, $A_k = (ik+\rho_k)/(2|\alpha_k|)$, $\varphi_k = \arg(\alpha_k)$, and $O_k = A_k(\sqrt{1-1/A_k^2}-1)$. The results hold if $|O_k|<1$, which is fulfilled during the flow. The set of flow equations (17)–(19) will be referred to as "fRG scheme I" in the following.

In the renormalization scheme for a translationally invariant system proposed by Andergassen *et al.*,[17] further approximations are made. The flow equations (11) for the interactions $U_{i;k}$ are Fourier transformed and then projected onto the Fermi surface, i.e., only momenta on the Fermi surface are considered during the flow. In contrast, such an approximation is not done in Eq. (19). Furthermore, the equation for $U_{i;k}$ is decoupled from the flow equations for the self-energies [see Eq. (10)] by using noninteracting self-energies. This leads to a flow equation, which can be solved analytically,

$$\dot{U}_k = -\frac{U_k^2}{4\pi^2 \sin^2 k_F} \sum_{\omega=\pm k} \int_0^{2\pi} dm \left[\frac{(\cos m - \cos k_F)^2}{(i\omega+\rho_0+2\alpha_0\cos m)^2} - \frac{[\cos m - \cos(2k_F)]^2}{[i\omega+\rho_0+2\alpha_0\cos(m+k_F)](i\omega+\rho+2\alpha\cos(m-k_F))} - \frac{2(\sin m \sin k_F)^2}{(-i\omega+\rho_0+2\alpha_0\cos m)(i\omega+\rho_0+2\alpha_0\cos m)} \right]. \tag{22}$$

One obtains[17]

$$U_k = \frac{U}{1-UH(k)} \tag{23}$$

with

$$H(k) = -\frac{k}{2\pi} + \frac{1}{\pi}\mathrm{Re}\left[\frac{(4-\mu_0^2)k^2 - 2i\mu_0(2-\mu_0^2)k + \mu_0^4 - 6\mu_0^2 + 8}{2(4-\mu_0^2)\sqrt{k^2 - 2i\mu_0 k + 4 - \mu_0^2}} - \frac{i\mu_0}{2}\sinh^{-1}\frac{k-i\mu_0}{2} + \frac{\mu_0^4}{2(4-\mu_0^2)^{3/2}}\tanh^{-1}\frac{4+\mu_0^2+i\mu_0 k}{\sqrt{(4+\mu_0^2+i\mu_0 k)^2 + 4(k-2i\mu_0)^2}} \right] \tag{24}$$

and $\mu_0 = -2\cos k_F$. The set of equations used by Andergassen *et al.*[17] will be referred to as "fRG scheme-II" in the following. The essential difference between both renormalization schemes is that the fRG scheme-II uses a Fermi-surface projection in the interaction renormalization.

Since the fRG is a grand canonical method, observables depend on the chemical potential μ via the initial conditions of the flow equations. However, in practice, we usually want to perform a calculation at fixed particle number or filling factor. At half-filling, the chemical potential is given by $\mu = U$ because of particle-hole symmetry. This is derived in the Appendix. For other filling factors, the chemical potential must be determined numerically.

To this end, we use the relation $N = -d\Omega/d\mu$ between the particle number N and the grand potential Ω at fixed temperature and volume. Therefore, the chemical potential can be determined from the condition

$$n_\mathrm{f} = -\frac{1}{L}\frac{\partial a_0(\mu)}{\partial \mu} \tag{25}$$

since $\Omega = a_{0,k=0}$. We will call a chemical potential obtained from this condition μ_1. At zero temperature, this can be rewritten as $\partial E_0(\mu)/\partial\mu = 0$ using the fact that $E_0 = a_0 + \mu N$.

Alternatively, one may use a condition based on Luttinger's theorem as proposed in Ref. 27: At zero temperature, the chemical potential equals the energy of a particle on the Fermi surface even in the presence of interactions. As a consequence, the renormalized self-energy on the Fermi surface is given by

$$\Sigma(k_F) = \Sigma(\pi n_\mathrm{f}) = \rho_{k=0} + 2\alpha_{k=0}\cos(\pi n_\mathrm{f}) = 0, \tag{26}$$

which provides a relation between the density n_f and the chemical potential μ, on which ρ and α depend via the initial conditions of the renormalization flow. We will call a chemical potential defined by this condition μ_2. (Note that in accordance with the definitions of the previous section, the self-energy contains the chemical potential as well as the free particle energy.) Technically, Eq. (26) is derived from the condition for the propagator G:

$$\sum_n G(k_n, t\to 0^-) = N. \tag{27}$$

In principle, in a completely consistent theory, both conditions (25) and (26) should produce the same results. However, fRG is not particle number conserving,[18] and the two conditions produce different results.[19,28] As a consequence, we may obtain two different values for the chemical potential. Therefore, it has to be decided which condition is more suitable for practical fRG calculations.

At zero temperature and in a particle-number-conserving theory, the quantity μ_3 defined by

$$\mu_3 = E(N+1) - E(N) \tag{28}$$

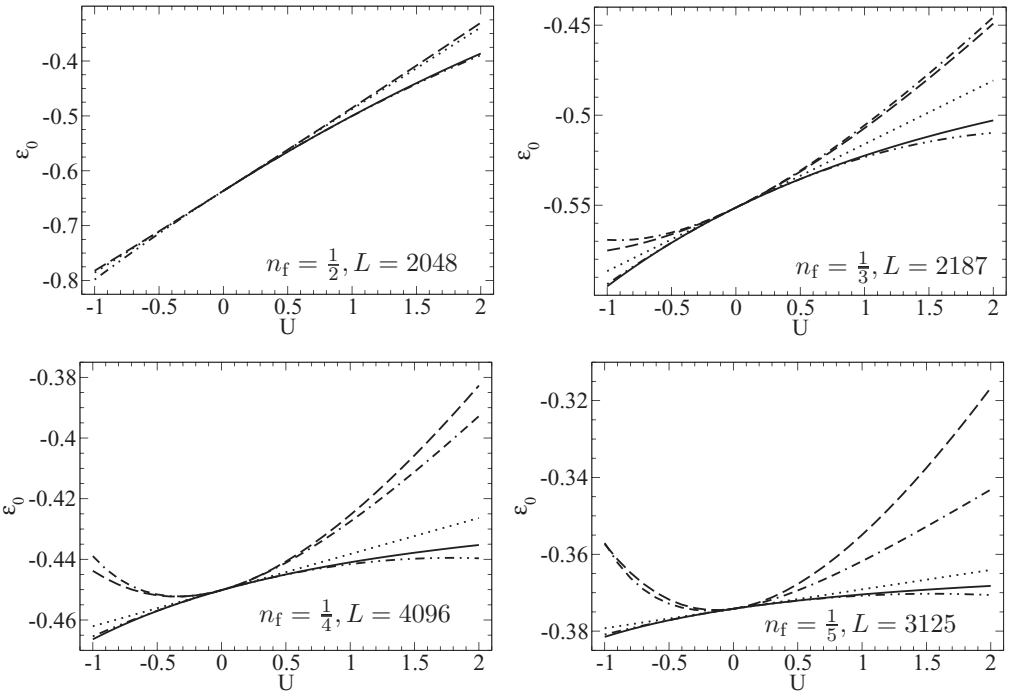

FIG. 1. Ground-state energy per site as a function of the interaction parameter U for filling $n_f = \frac{1}{2}, \frac{1}{3}, \frac{1}{4}, \frac{1}{5}$. Full line: finite-size Bethe ansatz; dotted line: first-order perturbation theory; double dotted dashed line: second-order perturbation theory; dashed line: fRG scheme-I; double dashed dotted line: fRG scheme-II. For half-filling, results of both fRG schemes agree numerically within the resolution of this figure.

should also agree with the chemical potential μ. In truncated fRG schemes, this is not the case, and Eq. (28) constitutes another way to numerically determine a chemical potential.

IV. RESULTS AND DISCUSSION

In this section, the ground-state energy and its finite-size dependence are determined numerically using the renormalization schemes developed in the previous section. We analyze the results in terms of the parameters of Eq. (2) and compare with numerical results from finite-size Bethe ansatz as well as perturbation theory. For convenience, a few necessary Bethe ansatz formulas are collected in the Appendix. The perturbative calculations are similar to Ref. 21.

We first discuss calculations of the ground-state energy per site ϵ_0. Figure 1 shows results for various filling factors calculated for relatively large systems (from 2048 up to 4096 sites) so that finite-size terms are negligible (increasing the system size by factor $1/n_f$ would change the energy per site ε_0 at the order of 10^{-5}). Both fRG schemes introduced in the previous section produce quantitatively similar results, which are, however, in slight disagreement with Bethe ansatz calculations particularly for larger interactions U. Second-order perturbation theory[21] agrees with Bethe ansatz results significantly better than fRG. At half-filling, fRG results resemble first-order perturbation theory. It is also interesting to observe that the differences between Bethe ansatz and perturbation theory decrease with decreasing filling factor, while the differences between Bethe ansatz and fRG are of similar size for all fillings investigated. This point is discussed further below.

Let us discuss possible reasons for these findings: As was explained in the previous section, the huge set of coupled ordinary differential equations, which is equivalent to the

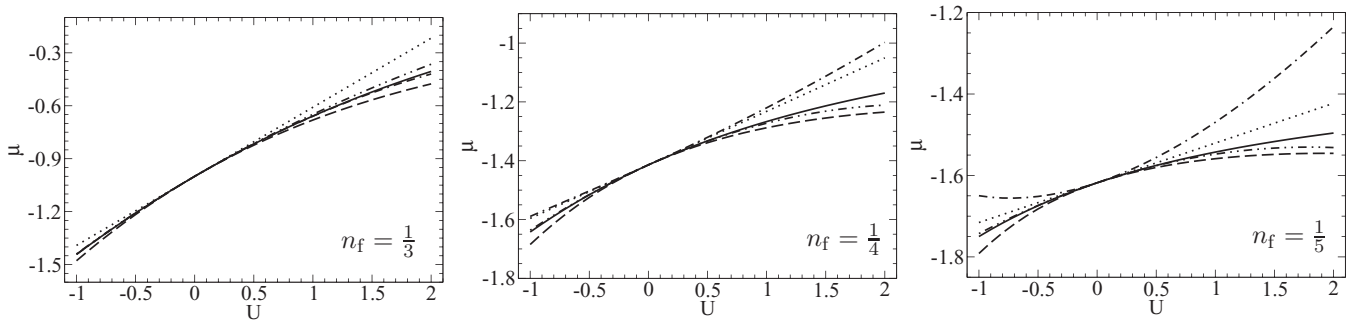

FIG. 2. Chemical potential as a function of the interaction parameter U for filling $n_f = \frac{1}{3}, \frac{1}{4}$, and $\frac{1}{5}$. For $n_f = \frac{1}{2}$, it holds that $\mu = U$. Plot symbols as in Fig. 1.

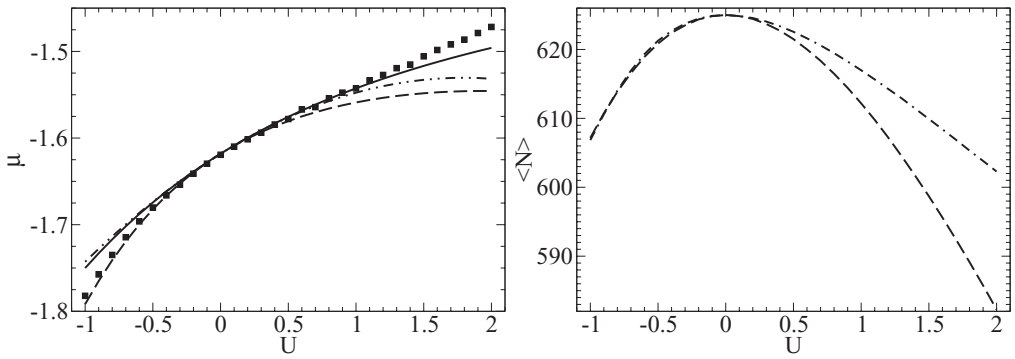

FIG. 3. Chemical potential (left) and number of particles (right) for filling $n_f = \frac{1}{5}$ as a function of the interaction parameter U. Plotting symbols as in Fig 1. The squares show results obtained using condition (25).

functional flow equation, is truncated at second order. (This is conventionally done to keep the calculation manageable.) Furthermore, it is assumed that the renormalization flow maintains the nearest-neighbor structure, and all longer-range terms, which may develop during the renormalization, are neglected. Additionally, one makes a static approximation. This procedure eliminates terms which are second order in the interaction[26] and explains differences between fRG and second-order perturbation theory. However, there is another issue which is particularly important away from half-filling: In order to obtain the ground-state energy, one needs to determine numerically the chemical potential μ as well as the particle number N for input into the initial condition (12) and the relation $E_0 = a_0 + \mu N$. Both μ and N can only be determined with numerical and systematic uncertainty, as will be discussed in the following. These uncertainties in μ and N are large enough to explain the differences between fRG and perturbation theory shown in Fig. 1. Consequently, a quantitative determination of ϵ_0 within the fRG approach is not easy. The advantage of fRG to be able to treat relatively large system sizes is offset by the mentioned difficulties due to the approximations involved.

An important ingredient of ground-state calculations away from half-filling is the chemical potential, which we now discuss separately. In the previous section, we introduced and discussed two different conditions in order to determine the chemical potential [Eqs. (25) and (26)]. In Fig. 2, we first present chemical potentials calculated from the self-energy using condition (26). We observe that, as expected from Ref. 21, second-order perturbation theory agrees rather well with Bethe ansatz calculations. The fRG scheme-I (dashed line) is also in quite good agreement with the Bethe ansatz. In contrast, the fRG scheme-II (used by Andergassen *et al.*) rather strongly disagrees even with first-order perturbation theory. This may be a consequence of the Fermi-surface projection employed in the fRG scheme-II.

To obtain the chemical potential from condition (25), the ground-state energy must be calculated as a function of μ. In the left panel of Fig. 3, we compare results using both conditions within fRG scheme-I for $n_f = \frac{1}{5}$. Quantitatively, the results produced by condition (25) are comparable to second-order perturbation theory. However, it turns out that if we relate particle number and ground-state energy via condition (25) within our fRG truncation scheme, then the parity conditions noted after Eq. (2) are not fulfilled. We finally note that in fRG scheme-I the quantity μ_3 defined in Eq. (28) is numerically equal to the chemical potential μ_1 [Eq. (26)]. In scheme-II, these two quantities are quite different, which is probably a consequence of neglecting the self-energy feedback in the renormalization of the interaction.

We may illustrate the inconsistencies observed between the two conditions (25) and (26) in another way: If we determine the chemical potential from Eq. (26), then the particle number calculated from Eq. (25) appears not to be conserved for different interaction strength.[19] For filling $n_f = \frac{1}{5}$, this is demonstrated in the right panel of Fig. 3: the calculated total number of particles is changing with the interaction strength (the correct value 625 can be read off the figure at $U = 0$).

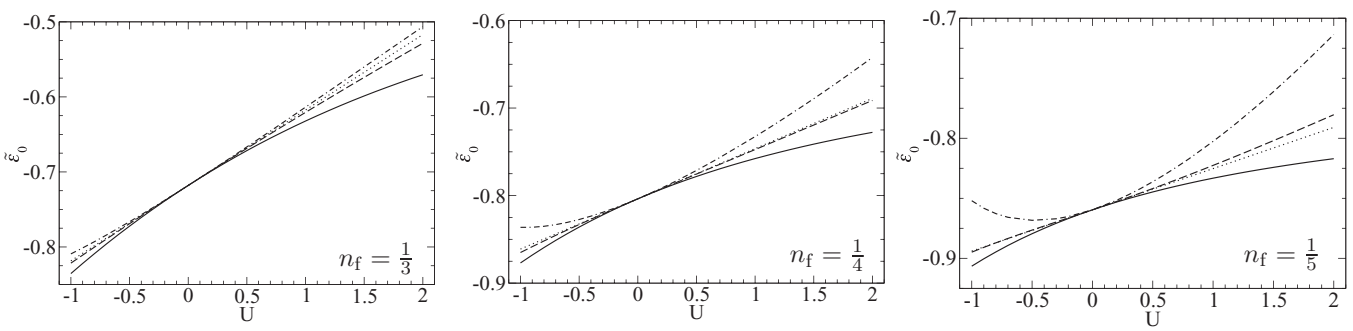

FIG. 4. The quantity $\widetilde{\varepsilon}_0 = \varepsilon_0 + (\frac{1}{2} - n_f)\mu$ as a function of the interaction parameter U for filling $n_f = \frac{1}{3}, \frac{1}{4}$, and $\frac{1}{5}$. Plotting symbols as in Fig. 1.

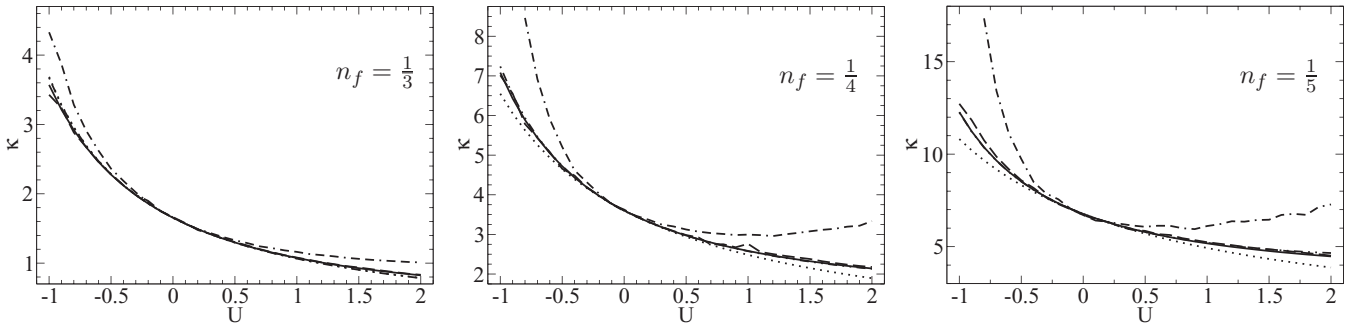

FIG. 5. Compressibility as a function of the interaction parameter U for filling $n_f = \frac{1}{3}, \frac{1}{4}$, and $\frac{1}{5}$. Plotting symbols as in Fig. 1.

Similar inconsistencies can be observed when the number of particles is calculated from condition (26) using μ_1. As a consequence, parity calculated using μ_1 is not conserved for different magnetic fluxes φ.

The initial condition for a_0 [Eq. (12)] and the relation between a_0 and the ground-state energy $E_0 = a_o + \mu N$ both depend on the chemical potential and the number of particles. As was just discussed in some detail, both these quantities can only be determined approximately within the fRG schemes (see Figs. 2 and 3). This in turn induces uncertainties for the determination of the ground-state energy per site ε_0. In order to investigate this influence, we define the quantity

$$\widetilde{\varepsilon}_0 = \varepsilon_0 + \left(\tfrac{1}{2} - n_f\right)\mu = \Omega/L + \mu/2, \tag{29}$$

which should be less sensitive to uncertainties in the chemical potential than ε_0 itself. Results for filling $n_f = \frac{1}{3}, \frac{1}{4}$, and $\frac{1}{5}$ are shown in Fig. 4. We observe that fRG results for $\widetilde{\varepsilon}_0$ within scheme-I are consistently in agreement with first-order perturbation theory. For ε_0, we observed similar behavior at half-filling, where the chemical potential can be determined exactly.

Next, we extract the compressibility κ from the finite-size dependence of the ground-state energy Eq. (2):

$$\frac{1}{\kappa} = \frac{N^2}{L}\frac{\partial^2 E_0}{\partial N^2} = \pi n^2 \frac{u}{K}. \tag{30}$$

Numerical results for this quantity are presented in Fig. 5. Again, one observes that fRG scheme-I appears to be quantitatively superior over fRG scheme-II. Here, fRG scheme-I is in very good agreement with second-order perturbation theory. Results obtained for the chemical potentials μ_1 and μ_2 in scheme-I agree numerically. Like the number of particles, also the compressibility (as an average of the density-density correlation function) should be obtained the same when calculated in momentum or real space. Therefore, the observed differences between the two fRG schemes can again be attributed to the Fermi-surface projection employed in scheme-II.

Finally, we present results for the Luttinger-liquid parameter K. This parameter may be extracted from the numerical calculations using different approaches. First, there is the relation to the finite-size dependence of the ground-state energy given in Eq. (2):

$$K = \pi N \sqrt{\frac{\kappa}{L}\frac{\partial^2 E_0}{\partial \varphi^2}}. \tag{31}$$

However, if the ground-state energy is not available as in the calculations in Ref. 16, one needs another way to determine K. In Ref. 16, it is proposed to use the relation

$$K = \sqrt{\frac{1 - g/(2\pi u)}{1 + g/(2\pi u)}}, \tag{32}$$

where g is a renormalized interaction. Details on the precise determination of g are given in Refs. 16 and 27. It is important to note that Eq. (32) is based on the Luttinger model. Just as for the chemical potential, one expects that due to the truncations involved in the different renormalization scheme formulas, Eqs. (31) and (32) do not produce the same results.

In Fig. 6, we present results based on Eq. (32). In order to bring out small differences, we here plot ΔK, i.e., the difference between Bethe ansatz results and various

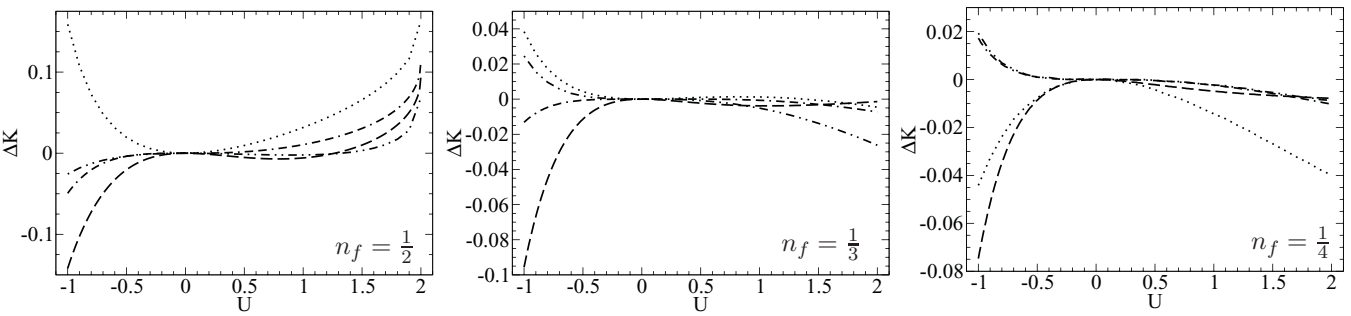

FIG. 6. Difference ΔK of the Luttinger parameter K calculated from Eq. (32) and finite-size Bethe ansatz as a function of the interaction parameter U for filling $n_f = \frac{1}{2}, \frac{1}{3}$, and $\frac{1}{4}$. Plotting symbols as in Fig. 1.

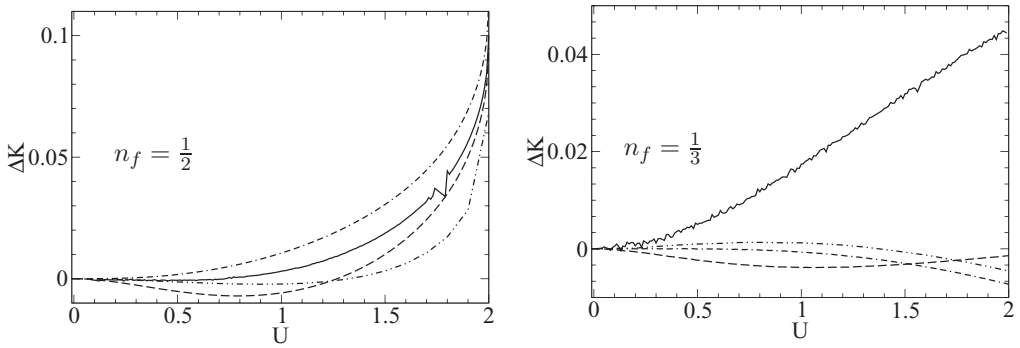

FIG. 7. Difference ΔK of the Luttinger parameter K calculated from Eq. (31) and finite-size Bethe ansatz as a function of the interaction parameter U for filling $n_f = \frac{1}{2}$ and $\frac{1}{3}$ (full line). For comparison, corresponding results of Fig. 6 are shown again with plotting symbols as in Fig. 1.

approximation schemes as a function of the interaction U and for various fillings. For the Luttinger parameter K, results of fRG scheme-II obviously agree better with Bethe ansatz than those of scheme-I. A fit in the U interval $(-1,2)$ indicates that scheme-II agrees with Bethe ansatz up to the second order in U, while scheme-I only agrees up to first order in U. This fact motivated the authors of Refs. 16 and 17 to prefer fRG scheme-II and its way to determine the interaction. They suggest that fRG scheme-II provides a better description of K due to its projection of the interaction on the Fermi surface. At half-filling, one observes an increasing ΔK for the large U interval, which may indicate the emergence of the phase transition to a charge density wave, which only occurs at half-filling.

Additionally, we show in Fig. 7 numerical results from fRG scheme-I for the Luttinger-liquid parameter K extracted from the flux dependence of the ground-state energy using Eq. (31). The figure indicates that one obtains results in good agreement with Bethe ansatz. Determination of the flux dependence of the ground-state energy is not easy for small (large) φ for even (odd) numbers of particle due to the ground-state degeneracy. Therefore, the flux dependence is determined only from numerical results for large (small) φ. Furthermore, we observe that determination of the φ dependence of the ground-state energy is very sensitive to the choice of k_0, the point where the numerical renormalization flow starts. This is indicated by the numerical noise seen in Fig. 7. One may reduce noise by increasing k_0. Moreover, the variation of the energy as a function of the magnetic flux is very small, and therefore a precise numerical determination of a derivative is difficult. Consequently, the second-order derivative of the energy with respect to the flux is numerically less precise than the second-order derivative with respect to number of particles.

Figure 7 demonstrates that K determined via Eq. (31) at half-filling produces in the U interval (0,0.75) the smallest ΔK of all methods. At smaller fillings, ΔK is rather large. We attribute this to the difficulties to determine the chemical potential, a problem we do not have at half-filling. Again, this problem is related to the nonconservation of particle number within the fRG approximation schemes. Since we have seen above that the compressibility is less affected by this problem, we conclude that the flux dependence suffers most from this problem. (This is due to the very small variation of the energy as a function of the magnetic flux.)

V. SUMMARY

We studied the ground-state energy of a ring of interacting spinless fermions using fRG, Bethe ansatz, and perturbation theory and introduced a method for the renormalization of the interaction. The proposed renormalization procedure is compared to the scheme introduced by Andergassen *et al.* in Ref. 16. The two methods differ in the Fermi-surface projection of the renormalized interaction. From the numerical results we extracted the ground-state energy per site ε_0, the chemical potential μ, the compressibility κ, as well as the Luttinger parameter K.

For the energy per site ε_0, we found that at half-filling, both fRG methods agree with first-order perturbation theory. For other fillings, the differences to Bethe ansatz are almost constant, while differences of perturbation theory and Bethe ansatz decrease with decreasing filling. If we (artificially) remove the explicit dependence on chemical potential via the definition of the quantity $\tilde{\varepsilon}_0$ [see Eq. (29)], the results of scheme-I also away from half-filling agree with first-order perturbation theory. This qualitatively also holds for scheme-II.

Because the truncated fRG does not conserve the particle number, different theoretically equivalent definitions of the chemical potential μ are not equivalent numerically. One has to choose which definition of the chemical potential is suitable for fRG calculations, and we compared two different ways to determine the chemical potential. It was shown that the chemical potential μ_2 determined from condition (26) produces the same compressibility as the chemical potential μ_1 obtained from (25), but it conserves parity, and one obtains a chemical potential μ_3 from Eq. (28), which agrees with μ_1. These are good reasons to prefer the chemical potential μ_2 based on the Luttinger theorem Eq. (26). The chemical potential calculated in this way is, however, less precise (determined by comparison with Bethe ansatz) than the one calculated from Eq. (25). A better value is obtained from Eq. (28).

Results for the compressibility κ are similar to results obtained from second-order perturbation theory. They agree

numerically for both chemical potentials μ_1 and μ_2. This and the equality of μ_3 for both chemical potentials shows that dependence of energy on number of particles is described in fRG as good as in second-order perturbation theory.

Two different methods are also investigated for the calculation of the Luttinger-liquid parameter K. The first method is based on the Luttinger model and Eq. (32). In this case, fRG scheme-II produces better results than scheme-I due to Fermi-surface projection. Presumably, this approximation treats interaction effects around the Fermi surface more accurately and results in a better description of K. The second method is based on the finite-size dependence of ground-state energy. At half-filling, this method is the most accurate for small interaction strengths U. At other fillings, calculations are hampered by the difficulty to calculate numerically the second-order derivative of the energy with respect to magnetic flux φ.

From a detailed analysis of the numerical results, we conclude that the Fermi-surface projection used in scheme-II is advantageous for the quantitative description of the Luttinger parameter K, but it is not helpful for calculations of the ground-state energy. This finding should be relevant for other fRG calculations which involve the ground-state energy, e.g., the determination of the interaction between two impurities by Wächter *et al.*[29] In general, we conclude that a *consistent* description of Luttinger physics with fermionic fRG appears to be difficult, which we mainly attribute to the nonconserving character of the fRG approximation scheme. Our results also demonstrate via the comparison with perturbation theory that the fRG schemes considered here are only controlled to leading order in the interaction, with the exception of the calculation of the parameter K in the fRG scheme proposed in Ref. 16 by Andergassen *et al.*, which appears to be controlled to second order in U. However, this is fortuitous due the judicious use of the Luttinger model within the construction of this approximation and only applies to the Luttinger parameter K.

ACKNOWLEDGMENTS

We would like to thank S. Andergassen, A. Gendiar, and V. Meden for useful discussions and correspondence.

APPENDIX

1. fRG equations in static approximation

a. Flow equations

After Fourier transformation, using the relations (8), the effective average action (5) takes the form

$$\begin{aligned}\Gamma_k[\phi^*,\phi] = \beta a_{0,k} &+ \sum_{i,n}(i\omega_n + a_{i,i;k})\phi^*_{i,n}\phi_{i,n} \\ &+ a_{i+1,i;k}\phi^*_{i+1,n}\phi_{i,n} + a_{i,i+1;k}\phi^*_{i,n}\phi_{i+1,n} \\ &+ \frac{1}{\beta}\sum_{i,n,m,l} U_{i;k}\phi^*_{i,n}\phi_{i,m}\phi^*_{i+1,l}\phi_{i+1,n+l-m}. \quad \text{(A1)}\end{aligned}$$

Because the Hamiltonian is Hermitian, for the self-energies it holds that $a_{ij} = a^*_{ji}$. For convenience, we define

$$\tilde{\Gamma}_k = \frac{1}{\beta}\sum_{i,n,m,l} U_{i;k}\phi^*_{i,n}\phi_{i,m}\phi^*_{i+1,l}\phi_{i+1,n+l-m}. \quad \text{(A2)}$$

The inverse propagator matrix $\Gamma^{(2)}_k$ has the structure

$$\Gamma^{(2)}_k = \begin{pmatrix}\Gamma_{\phi^*\phi} & \Gamma_{\phi^*\phi^*} \\ \Gamma_{\phi\phi} & \Gamma_{\phi\phi^*}\end{pmatrix} = \bar{\Gamma}^{(2)}_k + \tilde{\Gamma}^{(2)}_k, \quad \text{(A3)}$$

where the indices indicate derivatives with respect to ϕ_n and ϕ^*_n, respectively. This matrix is separated into two parts, one part $\bar{\Gamma}^{(2)}_k$, which does *not* contain Grassmann variables, and a second part $\tilde{\Gamma}^{(2)}_k$, which does contain Grassmann variables. From Eq. (A1), it is obvious that the matrix $\bar{\Gamma}^{(2)}_k$ is given by

$$\begin{aligned}\bar{\Gamma}^{(2)}_{k;n,n'} &= \begin{pmatrix}-(\mathbf{a}_k + i\omega_n\mathbf{E}) & 0 \\ 0 & (\mathbf{a}_k + i\omega_n\mathbf{E})^T\end{pmatrix}\delta_{n,n'} \\ &= \begin{pmatrix}-\mathbf{g}^{-1}(i\omega_n) & 0 \\ 0 & [\mathbf{g}^{-1}(i\omega_n)]^T\end{pmatrix}\delta_{n,n'}, \quad \text{(A4)}\end{aligned}$$

where $\mathbf{E}$ is identity matrix diag$(1,1,\ldots,1)$. From Eq. (A2), one can see that the matrix $\tilde{\Gamma}^{(2)}_k$ is neither block diagonal in the site indices nor diagonal in the Matsubara indices. However, since we are only interested in the static approximation, we only need to retain Grassmann variables with Matsubara index 0. In this case, $\tilde{\Gamma}^{(2)}_k$ has the following Matsubara index structure

$$\begin{aligned}(\tilde{\Gamma}_{\phi^*\phi})_{n,n'} &\propto \delta_{n,n'}, \quad (\tilde{\Gamma}_{\phi\phi^*})_{n,n'} \propto \delta_{n,n'}, \\ (\tilde{\Gamma}_{\phi^*\phi^*})_{n,n'} &\propto \delta_{n,-n'}, \quad (\tilde{\Gamma}_{\phi\phi})_{n,n'} \propto \delta_{n,-n'}.\end{aligned} \quad \text{(A5)}$$

Using these results, it is easy to see that the renormalization group equation (4) can be written in the form

$$\frac{\partial}{\partial k}\Gamma_k[\phi^*,\phi] = -\frac{1}{2}\mathrm{tr}\sum_n\left[\mathbf{S}_{k,nn}\sum_\ell(-1)^\ell\left(\tilde{\Gamma}^{(2)}_k\mathbf{G}_k\right)^\ell_{nn}\right] \quad \text{(A6)}$$

with

$$\mathbf{S}_k = \mathbf{G}_k\frac{\partial}{\partial k}\mathbf{R}_k, \quad \mathbf{G}^{-1}_k = \bar{\Gamma}^{(2)}_k + \mathbf{R}_k. \quad \text{(A7)}$$

The trace symbol indicates a summation over site indices only. When evaluating the matrix product $(\tilde{\Gamma}^{(2)}_k\mathbf{G}_k)^\ell$, it is crucial to observe Eq. (A5): whenever an off-diagonal block of $\tilde{\Gamma}^{(2)}_k$ is multiplied with one of the blocks of $\mathbf{G}_k$, e.g., $\mathbf{g}(i\omega_n)$, one obtains $\mathbf{g}(i\omega_{-n})$.

For zero temperature, $T \to 0$ and *after* the evaluation of the necessary matrix products as explained above, we can replace the sum over the Matsubara index n in Eq. (A6) by an integral

$$\sum_{n=-\infty}^{\infty} \to \frac{\beta}{2\pi}\int_{-\infty}^{\infty} d\omega \quad \text{(A8)}$$

with ($\omega_n \to \omega$ and $\omega_{-n} \to -\omega$).

Using a sharp cutoff regulator of the form

$$\mathbf{R}_{k,nn'} = \begin{pmatrix}-Ck\theta(k^2-\omega^2)\mathbf{E} & 0 \\ 0 & Ck\theta(k^2-\omega^2)\mathbf{E}\end{pmatrix}\delta_{nn'}, \quad \text{(A9)}$$

one can perform the integration over ω analytically with the help of the relation[12]

$$\delta(\omega - k) f[\theta(\omega - k)] \to \delta(\omega - k) \int_0^1 ds\, f(s). \quad \text{(A10)}$$

Comparing the coefficients of the various Grassmann structures on both sides of Eq. (A6), one obtains the flow equations (9) (from $\ell = 0$), (10) (from $\ell = 1$), and (11) (from $\ell = 2$) for the various running couplings given in the main text.

b. Initial conditions

In order to solve these equations, we need appropriate initial conditions. These are obtained from the Hamiltonian (1) or the bare action of the model. The initial condition for the effective average action could be up to term proportional to C obtained from the condition $\Gamma(\infty) = S_0$. At infinity, one finds from the Hamiltonian

$$a_{0;\infty} = 0, \quad \text{(A11)}$$

$$a_{ii;\infty} = -\mu \quad \text{(A12)}$$

$$a_{i,i+1;\infty} = -e^{-i\phi/L}, \quad \text{(A13)}$$

$$a_{i+1,i;\infty} = -e^{i\phi/L}, \quad \text{(A14)}$$

$$U_{i;\infty} = U. \quad \text{(A15)}$$

However, due to the fact that for a numerical solution of the flow equations we have to start the renormalization flow at a finite k_0, we must take care of the initial flow from ∞ to k_0 analytically.

Because of the discretization, we evaluate fields at slightly different times in the path integral $\bar{\phi}(\tau + \delta)$, $\phi(\tau)$ that introduce additional infinitesimal coefficients into our action

$$\begin{aligned}\Gamma[\phi^*_\alpha,\phi_\alpha] = \beta a_{0,k} &+ \sum_{i,n}(i\omega_n + a_{i,i;k}e^{-i\delta\omega_n})\phi^*_{i,n}\phi_{i,n} \\ &+ a_{i+1,i;k}e^{-i\delta\omega_n}\phi^*_{i+1,n}\phi_{i,n} \\ &+ a_{i,i+1;k}e^{-i\delta\omega_n}\phi^*_{i,n}\phi_{i+1,n} + \frac{1}{\beta}\sum_{i,n,m,l} U_{i;k}e^{-i\delta(\omega_n+\omega_l)} \\ &\times \phi^*_{i,n}\phi_{i,m}\phi^*_{i+1,l}\phi_{i+1,n+l-m}. \quad \text{(A16)}\end{aligned}$$

These coefficients regularize our equations at infinity, and we can integrate the flow from infinity to some value k_0. The flow of interaction U_i can be neglected because it depends on k as $1/k^2$ so we need to consider only self-energies and ground-state energy. For the ground-state energy and the diagonal part of the self-energy, we find the equations

$$\dot{a}_{0;k} = \frac{1}{2\pi}\sum_{\omega=\pm k} \ln k^{-n} \det(\mathbf{a} + ie^{i\omega\delta}\omega\mathbf{1}), \quad \text{(A17)}$$

$$\begin{aligned}\dot{a}_{ii;k} = \frac{1}{2\pi}\sum_{\omega=\pm k} &\left[U_{i-1}(\mathbf{a} + ie^{i\omega\delta}\omega\mathbf{1})^{-1}_{i-1,i-1}\right. \\ &\left. + U_i(\mathbf{a} + ie^{i\omega\delta}\omega\mathbf{1})^{-1}_{i+1,i+1}\right]. \quad \text{(A18)}\end{aligned}$$

For large k, they can be easily solved analytically:

$$\begin{aligned}a_{ii}(k_0) &= a_{ii}(\infty) - \frac{2U}{\pi}\int_\infty^{k_0} dk \frac{\sin(ik\delta)}{k} \\ &= U - \mu + \frac{2U}{\pi}\mathrm{Si}(k_0\delta) \quad \text{(A19)}\end{aligned}$$

from which we have

$$a_0(k_0) = -\frac{1}{\pi}\sum_j \int_\infty^{k_0} a_{jj;k}\frac{\sin(k\delta)}{k} \quad \text{(A20)}$$

$$= \frac{1}{2}\left(\frac{LU}{2} - L\mu\right) + \frac{1}{\pi}(\mu L - LU)\mathrm{Si}(k_0\delta) + \frac{UL}{\pi^2}\mathrm{Si}[(k_0\delta)^2] \quad \text{(A21)}$$

and initial conditions are obtained by performing limit $\delta \to 0^+$.

2. Determinant and inverse of a periodic tridiagonal matrix

In this Appendix, we study $L \times L$ Toeplitz matrices of the form

$$\mathbf{T} = \begin{pmatrix} d & a & 0 & \dots & a^* \\ a^* & d & a & & 0 \\ 0 & \ddots & \ddots & \ddots & \vdots \\ \vdots & & a^* & d & a \\ a & \dots & 0 & a^* & d \end{pmatrix}. \quad \text{(A22)}$$

Their normalized eigenvectors x_j and corresponding eigenvalues X_j are obtained as

$$\mathbf{x}_j = \frac{1}{\sqrt{L}}(e^{ik_j}, e^{i2k_j}, \dots e^{iLk_j}), \quad X_j = d + ae^{ik_j} + a^*e^{-ik_j} \quad \text{(A23)}$$

with $k_j = \frac{2\pi j}{L}$ for $j = 1, \dots, L$. The determinant of $\mathbf{T}$ is obtained as the product of all eigenvalues. The inverse of $\mathbf{T}$ reads as

$$(\mathbf{T}^{-1})_{mn} = \frac{1}{L}\sum_{j=1}^{L}\frac{e^{i(m-n)k_j}}{X_j}, \quad \text{(A24)}$$

and evaluation of the sum yields

$$\begin{aligned}(\mathbf{T}^{-1})_{mn} = \frac{e^{i(n-m)\varphi}}{d\sqrt{1-\frac{1}{A^2}}}&\left(O^{|m-n|} + O^{m-n}\frac{O^L e^{-iL\varphi}}{1 - O^L e^{-iL\varphi}}\right. \\ &\left. + O^{n-m}\frac{O^L e^{iL\varphi}}{1 - O^L e^{iL\varphi}}\right) \quad \text{(A25)}\end{aligned}$$

with $A = d/(2|a|)$, $\varphi = \arg(a)$, and $O = A(\sqrt{1 - 1/A^2} - 1)$. This result is valid for $|K| < 1$. From Eq. (A25), we can also read off the result for an infinite ring ($L \to \infty$)

$$\left(\mathbf{T}^{-1}_\infty\right)_{mn} = \frac{O^{|m-n|}}{d\sqrt{1-\frac{1}{A^2}}} \quad \text{(A26)}$$

and we can determine "finite-size effects."

3. Chemical potential at half-filling

In this Appendix, we use the definitions and notations introduced in Sec. II. For a lattice with an even number of sites, we define the unitary operator (see, e.g., Ref. 30)

$$J^{(sh)} = (c_L^+ - c_L)(c_{L-1}^+ + c_{L-1})\dots(c_2^+ - c_2)(c_1^+ + c_1) \tag{A27}$$

with the properties

$$\begin{aligned} J^{(sh)} c_j (J^{(sh)})^+ &= (-1)^j c_j^+, \\ J^{(sh)} c_j^+ (J^{(sh)})^+ &= (-1)^j c_j. \end{aligned} \tag{A28}$$

This operator defines the so-called Shiba transformation. If we act with this operator on a vacuum state $|0\rangle$ (empty lattice), we obtain

$$J^{(sh)}|0\rangle = c_L^+ \dots c_1^+ |0\rangle, \tag{A29}$$

i.e., it maps an empty lattice onto a fully occupied lattice. Consequently, a lattice with N occupied states is mapped onto a lattice with $L - N$ occupied states.

For simplicity, we only discuss the magnetic field free case and set $\phi = 0$ in the Hamiltonian H. Then, $H - \mu\hat{N}$ transforms as

$$J^{(sh)}(H - \mu\hat{N})(J^{(sh)})^+ = H + (U - \mu)L + (\mu - 2U)\hat{N} \tag{A30}$$

under a Shiba transformation ($\hat{N}$ is the number operator). The Gibbs free energy of the system

$$F(\mu,T,U) = -T \ln \left[\mathrm{tr} \exp\left(-\frac{H(U) - \mu\hat{N}}{T} \right) \right] \tag{A31}$$

is invariant under the unitary Shiba transformation

$$F(\mu,T,U) = L(U - \mu) + F(2U - \mu,T,U) \tag{A32}$$

since the trace is invariant under cyclic permutations of operators.

The expected number of electrons $N = \langle \hat{N} \rangle$ in the system is then determined from

$$N = -\frac{\partial}{\partial \mu} F(\mu,T,U) = L + \frac{\partial}{\partial \mu'} F(\mu',T,U)\Big|_{\mu'=2U-\mu}. \tag{A33}$$

Consequently,

$$L - N = -\frac{\partial}{\partial \mu'} F(\mu',T,U)\Big|_{\mu'=2U-\mu} \tag{A34}$$

from which follows

$$\mu[1 - n_f] = 2U - \mu[n_f]. \tag{A35}$$

Therefore, at half-filling, it holds that $\mu = U$.

4. Bethe ansatz

Here, we briefly review some Bethe ansatz formulas used for our calculations. We follow standard presentations as, e.g., given in Ref. 1, where more details can be found. The ground-state wave function $|\psi\rangle$ of the Hamiltonian (1) ($t = 1$) is assumed to have the following form ("Bethe ansatz"):

$$|\psi\rangle = \sum_{j_1 < j_2 < \dots < j_N} \sum_P A(P) e^{i \sum_m^N k_{P_m} j_m} |j_1 \dots j_N\rangle, \tag{A36}$$

where P represents all permutations of the index set $\{1,\dots,N\}$. Then, the ground-state energy E_0 of the Hamiltonian is given by

$$E_0 = -2 \sum_{i=1}^N \cos k_i, \tag{A37}$$

and the parameters k_i solve the set of nonlinear equations

$$k_i L = 2\pi n_i - \phi + \sum_j \Theta(k_i,k_j), \tag{A38}$$

where n_i is integer if N is odd and half-integer if N is even. The phase $\Theta(k_i,k_j)$ is defined by

$$\Theta(k_i,k_j) = 2\,\mathrm{arctg} \frac{U \sin\left(\frac{k_i - k_j}{2}\right)}{2\cos\left(\frac{k_i + k_j}{2}\right) + U \cos\left(\frac{k_i - k_j}{2}\right)}. \tag{A39}$$

This set of equations can be solved easily numerically for given N and U. Then, with the numerically determined parameters k_i, one calculates the ground-state energy, the chemical potential $\mu = \partial E_0 / \partial N$, and the LL parameters.

*michael.weyrauch@ptb.de

[1] T. Giamarchi, *Quantum Physics in One Dimension* (Clarendon, Oxford, UK, 2004).
[2] A. M. Tsvelik, *Quantum Field Theory in Condensed Matter Physics* (Cambridge University Press, Cambridge, UK, 2003).
[3] F. D. M. Haldane, Phys. Rev. Lett. **45**, 1358 (1980).
[4] H. W. J. Blöte, J. L. Cardy, and M. P. Nightingale, Phys. Rev. Lett. **56**, 742 (1986).
[5] C. L. Kane and M. P. A. Fisher, Phys. Rev. Lett. **68**, 1220 (1992).
[6] C. L. Kane and M. P. A. Fisher, Phys. Rev. B **46**, 15233 (1992).
[7] E. Wong and I. Affleck, Nucl. Phys. B **417**, 403 (1994).
[8] S. R. White, Phys. Rev. Lett. **69**, 2863 (1992).
[9] S. Qin, M. Fabrizio, L. Yu, M. Oshikawa, and I. Affleck, Phys. Rev. B **56**, 9766 (1997).
[10] V. Meden, P. Schmitteckert, and N. Shannon, Phys. Rev. B **57**, 8878 (1998).
[11] C. Wetterich, Phys. Lett. B **301**, 90 (1993).
[12] T. R. Morris, Int. J. Mod. Phys. A **9**, 2411 (1994).
[13] M. Salmhofer and C. Honerkamp, Prog. Theor. Phys. **105**, 1 (2001).
[14] W. Metzner, M. Salmhofer, C. Hohnercamp, and V. Meden, Rev. Mod. Phys. **84**, 299 (2012).
[15] V. Meden, W. Metzner, U. Schollwöck, and K. Schönhammer, Phys. Rev. B **65**, 045318 (2002).
[16] S. Andergassen, T. Enss, V. Meden, W. Metzner, U. Schollwöck, and K. Schönhammer, Phys. Rev. B **73**, 045125 (2006).

[17]S. Andergassen, T. Enss, V. Meden, W. Metzner, U. Schollwöck, and K. Schönhammer, Phys. Rev. B **70**, 075102 (2004).
[18]T. Enss, Ph.D. thesis, Max-Planck-Institute für Festkrperforschung, Stuttgart, 2005, e-print arXiv:cond-mat/0504703.
[19]G. Baym, Phys. Rev. **127**, 1391 (1962).
[20]H. Bethe, Z. Phys. A **71**, 205 (1931).
[21]K. Sano, J. Phys. Soc. Jpn. **69**, 1000 (2000).
[22]R. P. Feynman, Phys. Rev. **56**, 340 (1939).
[23]V. Meden and U. Schollwöck, Phys. Rev. B **67**, 035106 (2003).
[24]M. Weyrauch and D. Sibold, Phys. Rev. B **77**, 125309 (2008).
[25]J. Berges, N. Tetradis, and C. Wetterich, Phys. Rep. **363**, 223 (2002).
[26]C. Karrasch, T. Enss, and V. Meden, Phys. Rev. B **73**, 235337 (2006).
[27]S. Andergassen, Ph.D. thesis, Max-Planck-Institute für Festkrperforschung, Stuttgart, 2006, e-print arXiv:cond-mat/0603341.
[28]G. Baym and L. P. Kadanoff, Phys. Rev. **124**, 287 (1961).
[29]P. Wächter, V. Meden, and K. Schönhammer, Phys. Rev. B **76**, 045123 (2007).
[30]F. Essler, H. Frahm, F. Göhmann, A. Klümper, and V. Korepin, *The One-Dimensional Hubbard Model* (Cambridge University Press, Cambridge, UK, 2005).